MODELS AND METHODOLOGY FOR THE CHARACTERIZATION OF SURFACE-BREAKING CRACKS USING AN ULTRASONIC NEAR-FIELD SCATTERING MEASUREMENT

John C. Aldrin[1], Jeremy Knopp[2], James L. Blackshire[2], Shamachary Sathish[3]

[1]Computational Tools, Gurnee, IL 60031, USA
[2]Air Force Research Laboratory, Materials and Manufacturing Directorate, Wright-Patterson AFB, OH 45433, USA
[3]University of Dayton Research Institute, Dayton, OH 45469, USA

Abstract. Measurements using laser interferometry have been performed to study the displacement response of Rayleigh waves in close proximity to a surface-breaking crack. To gain a better understanding, numerical models for both infinite and finite crack cases were developed. Regions of intensification and decay were found to be highly localized around the crack site, and offer an advanced NDE technique for flaw characterization. Potential near-field measures were proposed and evaluated with respect to variation in crack depth and angle.

INTRODUCTION

A variety of techniques incorporating far-field measurements of the scattered field for an incident Rayleigh wave by a surface-breaking crack have been used to characterize crack depth [1]. For small cracks relative to the wavelength, amplitude measurements of the reflected and transmitted signals can be used to evaluate crack depth. A self-calibrating ultrasonic technique has also been demonstrated where the ratio of transmission to reflection coefficients can be obtained for use in crack sizing [2]. The time of flight diffraction (TOFD) technique performs large crack sizing through measurement of the difference in time between the reflected and the crack tip diffraction signals. Frequency domain methods such as surface wave spectroscopy have also been investigated. However, these techniques are often limited to a specific range of crack sizes (small or large cracks relative to wavelength) and are sensitive to variations in crack angle and crack face contact conditions. Also, since these techniques rely upon far-field measures, they do not provide quantitative information about the local characteristics of a crack.

Near-field measurements, to a lesser degree, have been investigated for nondestructive evaluation of crack depth. Vu and Kinra studied both the far-field and the near-field response using PZT transducers with wedges to generate and receive surface waves [3]. In this study, features were observed in both the near-field and far-field that were correlated with crack size. To improve the accuracy and localization of these near-field measurements, the use of laser interferometry has been explored. Jungerman et al. demonstrated the use of optical methods incorporating laser interferometry for the measurement of displacements associated with the scattering of Rayleigh waves from surface defects [4]. Transient near-field response measurements for an incident Rayleigh wave were made for a single small notch case and the concept of using the near-field displacement response for sizing was suggested. A fully non-contacting technique incorporating laser ultrasonic generation and laser interferometry measurements in close

proximity to surface-breaking cracks was studied by Cooper et al. for varying flaw size [5]. In a recent work by Blackshire and Sathish, the intensification of the ultrasonic field for an incident Rayleigh wave on a surface-breaking crack was observed experimentally through a near-field surface displacement measurement using a scanning laser interferometer [6]. Using this approach, a method for imaging the crack surface profile was demonstrated and a idea of localized crack characterization was proposed. A related approach is the scanning laser source technique, whereby a laser source is scanned over a region of interest and a far-field contact transducer measurement is made for crack detection and potential sizing [7,8].

To gain a better physical understanding of these near-field measurements, the use of modeling is proposed. Over the years, there have been a variety of analytical and numerical methods developed to address the problem of scattering from corners and surface breaking cracks [9-11]. However, the application of such models to address accurate near-field measurements of the scattered field from cracks and corners has been limited in scope. Prior modeling work has investigated the scanning laser source technique where the laser source is moved across the crack [12,13]. In this paper, 2D laser interferometric measurement models of the near-field scattering of surface waves from both corners and surface-breaking cracks are developed using both the finite element method (FEM) and the boundary element method (BEM). Studies were performed to evaluate the sensitivity of the near-field response to variation in crack depth and crack angle. Lastly, potential near-field measures of crack depth are evaluated for expanded range and improved accuracy with respect to far-field measures.

NEAR-FIELD SCATTERING RESPONSE AT A CORNER

Near-field scattering from a corner was investigated to provide insight into the scattering response for very large cracks through study of this more basic geometric problem. Two numerical methods, the finite element method and the boundary element method, were selected due to their capability to accurately calculate the scattering of surface waves from corners and cracks. The FEM package FEAP was used to solve the 2D finite element problem [14]. An implicit time domain FEM formulation was used to insure best accuracy. A description of the frequency domain BEM formulation has been previously presented [15]. A block diagram for this problem is shown in Figure 1(a). The material properties of aluminum (7075-T6) were used for the study. Traction free boundary conditions were applied to the surfaces of the block and the two bottom corners were fixed. A point source on the top surface was used to approximate the generation of incident Rayleigh waves at the corner. Careful attention to the distance between the source and corner was given in order to minimize the impact of surface skimming longitudinal waves and subsurface waves on the measurement results. The input response for the point source is given in Figures 1(b) and 1(c) for both the time and frequency domain respectively. A short pulse with a 5 MHz center frequency was used for the study. Discretization of the domain was increased beyond what is typically required for stability of the solution in order to accurately represent the complex scattering features near the corner. The results presented here for both FEM and BEM were found to converge with increased discretization.

Scanning laser interferometry has the capability to rapidly acquire the displacement response in time over a two dimensional region of a sample. However for visualization purposes, the maximum peak to peak displacement at each scan location is typically calculated and displayed. Thus, of primary interest in this study is to evaluate the available features of the maximum peak to peak measurements for crack characterization. Figure 2(a) displays the maximum normalized peak to peak displacement response near a corner

in the x and y directions calculated using 2D FEM. All displacement plots are normalized with respect to the maximum peak to peak vertical displacement of the incident Rayleigh wave. The displacement features exhibited in both the vertical and horizontal directions are the result of the interference of multiple waves incident to and scattered by the corner. The significant peak at the corner is due to the constructive interference of the incident surface wave, the reflected surface wave along the top surface, the transmitted surface wave along the side surface, and diffracted waves into the bulk medium. Moving away from the corner in the negative x direction, the measured vertical displacement peak drops significantly while the horizontal displacement peak falls off less rapidly. These general trends are related to the sub-surface displacement profile of a Rayleigh wave, where given the traction free boundary conditions, the sub-surface component of the transmitted surface wave will contribute to the measured displacements on the top surface. Moving further from the corner, a region of destructive interference primarily consisting of the incident and reflected surface waves is observed with maximum normalized peak to peak displacement values less than one. As expected for the short pulse case, moving further in the negative x direction will result in vertical displacments that approach one corresponding to the incident signal.

Figure 2(b) displays a comparison of the maximum normalized peak to peak displacement response near a corner in the measurement (y) direction for 2D FEM, 2D BEM and experimental results. A detailed description on the experimental setup and procedure used for the acquisition of the experimental data has been previously presented [6]. The agreement between the two numerical methods was good. For the two numerical methods and the experimental data, the agreement was good with the exception of very near to the corner. Given the agreement between the two numerical methods, potential sources of this difference very near the corner could be contributed to the experimental conditions. Such sources may include the laser spot size, the curvature and angle of the corner, and averaging that could potentially smooth the results. Additional work is necessary to validate this claim.

Figure 3 displays a comparison of the maximum normalized peak to peak displacement for varying corner angle from 70º - 110º. The maximum displacement response was found to be highly sensitive to changes in the corner angle from 90º. With decreasing the corner angle, the peak response at the corner was found to increase significantly, the slope of the curve from the corner was found to increase to a smaller degree, and the location of the local minimum was found to shift away from the corner. These trends provide an indication that the near-field displacement measurement can provide quantitative data for the determination of the angle for corners and potentially for the near edge of a large surface breaking crack. Additional features related to the near crack edge angle will be investigated in the next sections.

NEAR-FIELD SCATTERING RESPONSE AT A NOTCH

A block diagram of the scattering problem for the notch case with depth, d, and crack angle, θ, is shown in Figure 4. To simplify the numerical formulation for this initial study, an open notch was used. All simulated results presented for the notch case were performed with FEAP using a 2D FEM formulation [14]. The material properties, source parameters, and boundary conditions were set to be the same as for the corner scattering problem in the previous section.

Figure 5 displays the maximum normalized peak to peak vertical displacement response for measurement locations in close proximity to a surface breaking notch for varying notch depth. The crack depth values presented in the plot were normalized with respect to the

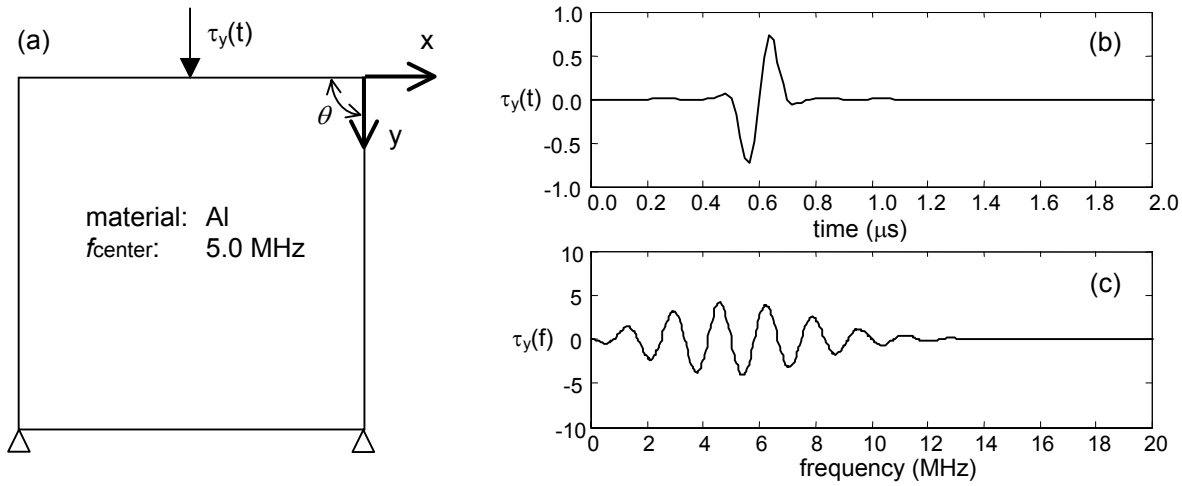

FIGURE 1. (a) Model diagram for the near-field scattering problem at a corner and plots of the input response for a short pulse as a function of (b) time and (c) frequency.

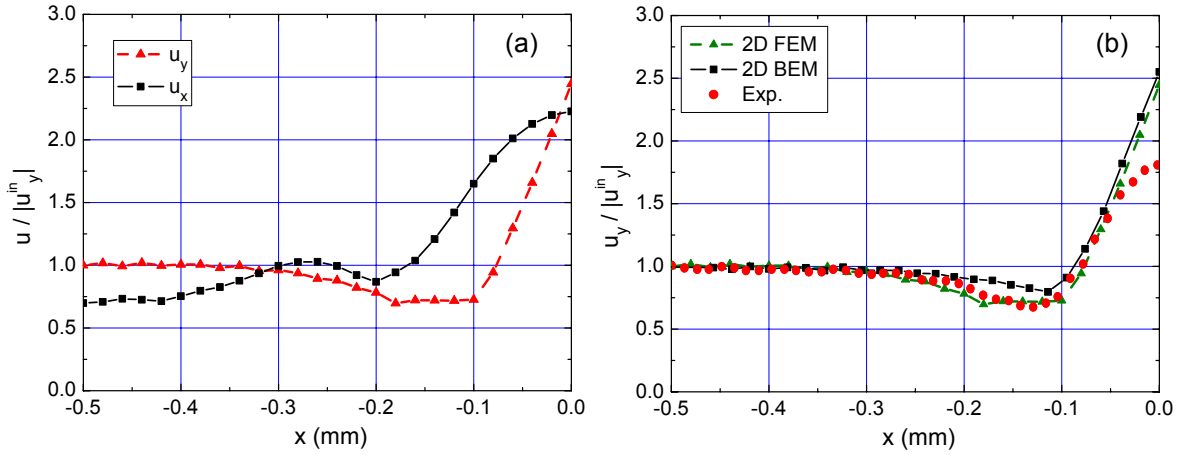

FIGURE 2. Plot of maximum normalized peak to peak displacement response near a corner (a) in the x and y directions using 2D FEM and (b) a comparison in y for 2D FEM, 2D BEM, and experimental results.

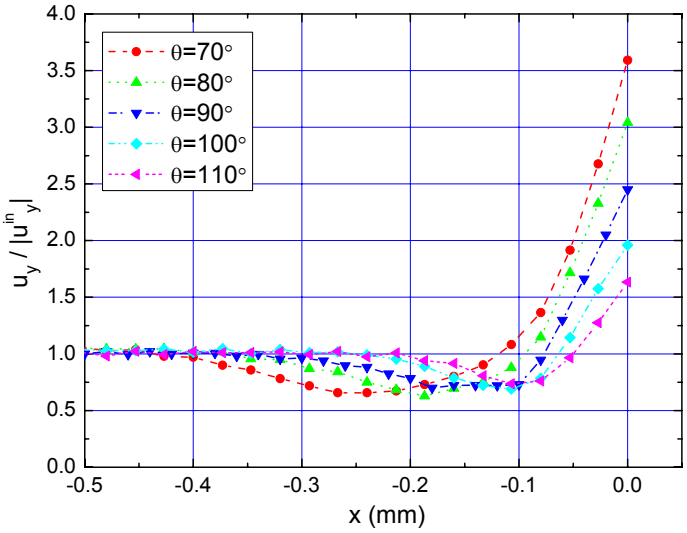

FIGURE 3. Plot of maximum normalized peak to peak displacement response near a corner in the y (vertical) direction for varying corner angle using 2D FEM.

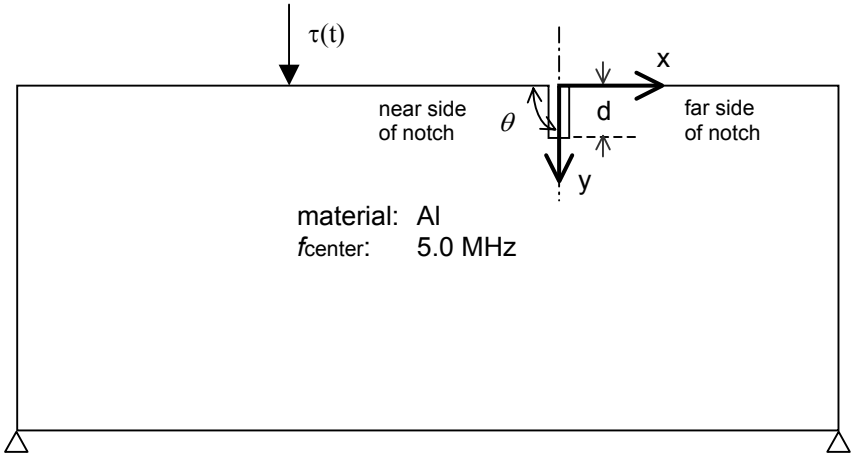

FIGURE 4. Model diagram for the near-field scattering problem from a surface-breaking notch.

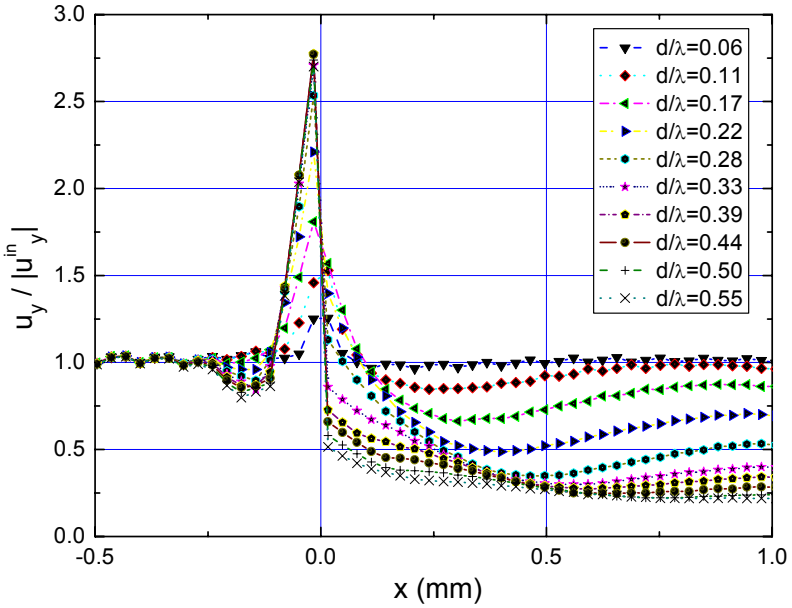

FIGURE 5. Plot of maximum normalized peak to peak displacement response near a surface breaking notch in the y (vertical) direction for varying notch depth using 2D FEM.

wavelength of the surface wave. The crack angle for this study was fixed at 90º. Several comments can be made about the nature of the displacement response with respect to crack depth. As the notch depth is increased, the maximum response at the near crack surface corner (relative to the incident wave source) initially increases due to changes in magnitude of the waves that contribute to the locally constructive interference. However, for larger flaws, the general characteristics of the displacement response becomes analogous to the case of an infinite crack resulting in a similar displacement response as observed in the previous section for the corner problem. On the far side of the notch (relative to the incident wave source) a general decay of the maximum displacement is observed with increasing notch depth. This decaying of the maximum displacement with notch depth is not evenly distributed over this region, but exhibits local regions of greater changes for different ranges of notch size. This can be contributed to the varying constructive and deconstructive interference from primarily two sources, transmitted waves along the notch faces and diffracted wave from the notch tip. These localized regions of intensification on

the near side of the notch and decay on the far side of the notch have been previously proposed through experimental studies as a means for enhanced crack detection [3,6].

METHODOLOGY FOR CRACK CHARACTERIZATION

Based on the observations from the previous section, three potential near-field measures for crack characterization are proposed. A plot shown in Figure 6(a) displays the features that these measures are based.

The first proposed measure (1) corresponds to the measurement of the maximum response at the near crack surface corner. Figure 6(b) plots measure 1 for varying notch depth. Initially, this measure increases in a generally linear fashion with notch depth primarily due to the constructive interference of the linearly growing reflected surface wave and the incident surface wave. This characteristic for small crack depths is similar in form to the far-field measurement of the reflection coefficient [11]. For larger notch sizes with shorter pulse widths, this measure essentially stabilizes when the tip diffraction signals no longer contribute to the point in time of the maximum response.

The second proposed measure (2) corresponds to the measurement of the minimum response on the near side of crack surface. Figure 6(c) plots measure 2 for varying notch depth. A consistent downward trend is observed for flaws varying from a value of d/λ of 0.2 to 0.6. This measure 2 has the potential to complement measure 1 to ideally expand the viable range for crack sizing beyond what can consistently be performed using far-field measures.

The third proposed measure (3) corresponds to an RMS measure of the maximum displacement over a range of measurement points on the far side of the notch. Figure 6(d) plots measure 3 for varying notch depth. A range of points from x = 0.0 mm to 1.0 mm are used for the calculation, but note that the ideal range is dependent upon the frequency of the ultrasonic signal. As with measure 2, a consistent downward trend is observed for flaws varying from a value of d/λ from 0.2 to 0.6. Measure 3 will likely be more reliable then measure 2 due to a greater sensitivity in the measure values for the same range of flaw sizes. As opposed to the far-field measurement of the transmission coefficient, where local minima are observed for a value of d/λ less than 0.5 [11], no local minima are observed for crack depths out to 0.6. This is due to the use of multiple data points in the calculation that smooth out the response due to the varying interference from the transmitted waves along the notch faces and the diffracted wave from the notch tip.

As previously discussed, notch angle was found to be a sensitive parameter of the near-field response for the corner case. Investigations were also performed for variation in crack angle and crack depth on these proposed measures. Figure 7(a) presents the results for measure 1, associated with the measurement of the maximum response at the near crack surface corner. Clearly, as observed for the corner case, there is a significant sensitivity of measure 1 to crack angle. Figure 7(b) presents the results for measure 3, associated with an RMS measure on the far side of the notch. Clearly, the signals on the far side of the notch were found to not have the sensitivity to variation in crack angle as the signals on the near side of the notch.

Based on these results, one can conjecture that a potential exists for both crack depth and crack angle characterization with the use of multiple near-field measure. Such capability for crack characterization does not exist with the use of far-field measurements. Based on these studies of potential near-field measures, a preliminary methodology for the sizing of surface-breaking cracks using these measures is proposed. The use of classification algorithms such as neural networks is suggested to perform the final task of quantifying crack depth and crack angle.

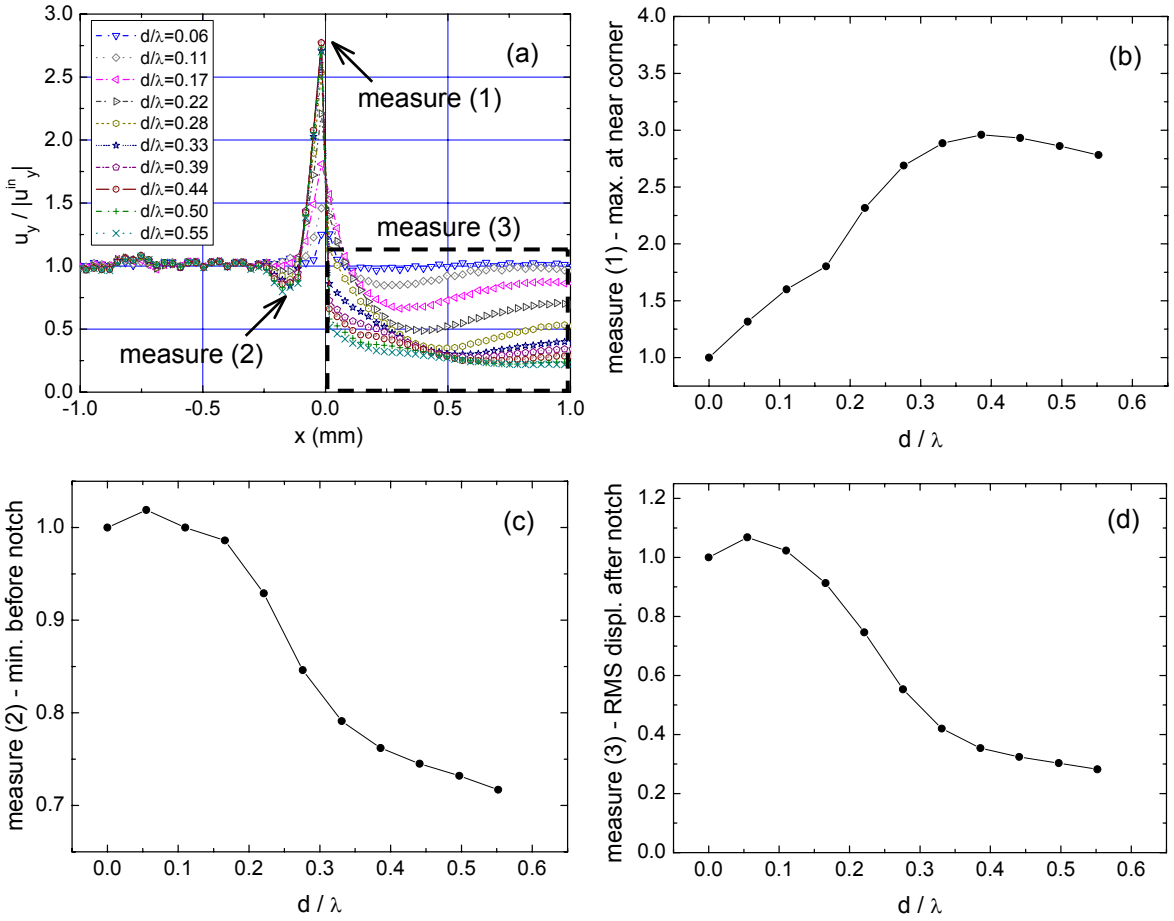

FIGURE 6. Plot of measures for crack characterization as a function of notch depth (a) displaying the association of measures (1-3) with near-field displacement measurements, (b) for measure 1 of maximum vertical displacement at near corner of notch, (c) for measure 2 of minimum vertical displacement before notch, d) for measure 3 of RMS displacement measurement for the region after the notch.

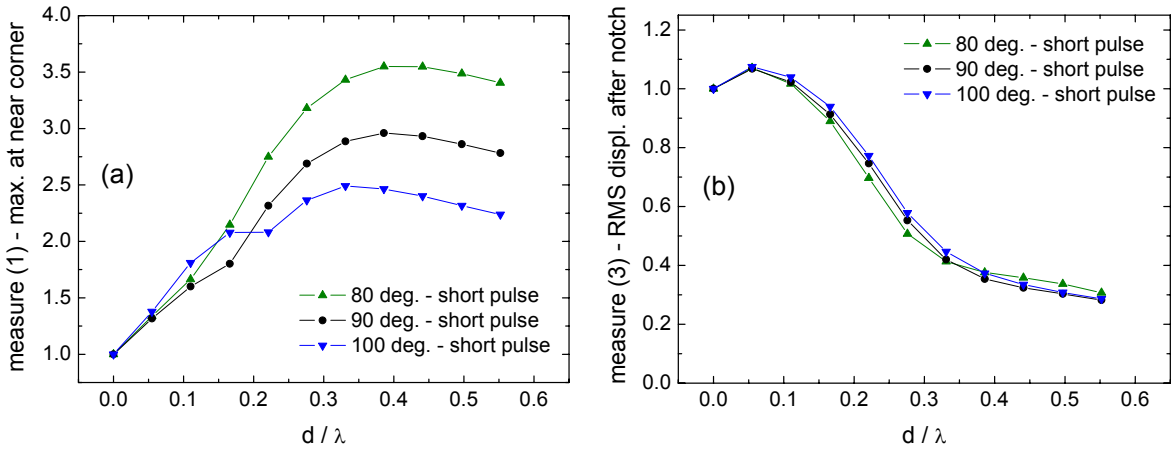

FIGURE 7. Plot of measures for crack characterization as a function of notch depth and notch angle with surface for (a) measure 1 of maximum vertical displacement at near corner of notch, and (b) measure 3 of RMS displacement measurement for region after notch.

CONCLUSIONS AND RECOMMENDATIONS

Through simulated studies, regions of intensification and decay were found to be highly localized around the crack site and offer an advanced NDE technique for detecting and characterizing surface-breaking cracks. Good agreement was found between the experimental and simulated data. The use of three measures to characterize flaw depth and corner angle was demonstrated. A discussion was also presented on the improvements of this methodology over existing far-field techniques for sizing surface-breaking cracks.

Although a methodology for the characterization of surface-breaking cracks has been demonstrated, additional work is required to both refine and validate this approach for practical applications. First, experimental validation of the methodology is needed. Second, improved models are required to address realistic ultrasonic source and crack topology conditions. Models would be beneficial for a design incorporating a laser line source to best generate the incident field without contact with the sample. Accurate but computationally efficient models are also needed to investigate issues related to the complex 3D scattering problem along the crack face. Changes in the local beam angle of incidence due to variation in local crack geometry, multiple reflections between the crack surfaces, and variation in crack surface contact conditions can impact in the near-field measurement results. There are indications from preliminary experimental studies that features related crack geometry and contact condition can be measured. Ideally, it would be beneficial to enhance the methodology by incorporating these measurement features and models using an inverse method approach.

ACKNOWLEDGEMENTS

The authors would like to acknowledge support for this study provided by AFRL-MLLP, Wright Patterson AFB OH.

REFERENCES

1. Doyle, P. A., Scala, C. M., *Ultrasonics*, **16**, 164-170, (1978).
2. Achenbach, J. D., Komsky, I. N., Lee, Y. C., Angel., Y. C., *J. NDE*, **11**, 103-108, (1992).
3. Vu , B. Q., Kinra, V. K., *J. Acoust. Soc. Am.*, **77**, 1425-1430 (1985).
4. Jungerman, R. L., Khuri-Yakub, B. T., Kino, G. S., *Mater. Eval.*, **42**, 444-450 (1984).
5. Cooper, J. A., Crosbie, R. A., Dewhurst, R. J., McKie, A. D. W., Palmer, S. B., *IEEE Ultra. Ferro. Freq. Cntrl.*, **5**, 462-470 (1986).
6. Blackshire, J. L., Satish, S., *Applied Physics Letters*, **80**, 3442-3444 (2002).
7. Kromine, A. K., Fomitchov, P. A., Krishnaswamy, S., Achenbach, J. D., *Mater. Eval.*, **58**, 173-177, (2000).
8. Yan, Z., Nagy, P., *NDT&E Int.*, **33**, 213-223, (2000).
9. Budaev, B. V., Bogy, D. B., *Wave Motion*, **22**, 239-257 (1995).
10. Bond, L. J., *Ultrasonics*, **17**, 71-77, (1979).
11. Angel, Y. C., Achenbach, J. D., *J. Acoust. Soc. Am.*, **75**, 313-319, (1984).
12. Sohn, Y., Krishnaswamy, S., *Ultrasonics*, **29**, 543-551, (2002).
13. Arias, I., Achenbach, J. D., *Review of Progress in QNDE*, **22**, 281-288, (2003).
14. Taylor, R. L., *FEAP - A Finite Element Analysis Program, Theory Manual*, University of California, Berkeley, http://www.ce.berkeley.edu/~rlt.
15. Song, W.-J., Popovics, J. S., Aldrin, J. C., Shah, S. P., *J. Acoust. Soc. Am.*, **113**, 717-725, (2003).